Temperature effect on colloidal PbSe quantum dot-filled liquid-core optical fiber

Hua Wu,[1] Yu Zhang,[1,2,*] Long Yan,[1] Yongheng Jiang,[2] Tieqiang Zhang,[2] Yi Feng,[2] Hairong Chu,[3] Yiding Wang,[1] Jun Zhao,[4] and William W. Yu[1,4,5]

[1]*State Key Laboratory on Integrated Optoelectronics, and College of Electronic Science and Engineering, Jilin University, Changchun 130012, China*

[2]*State Key Laboratory of Superhard Materials, and College of Physics, Jilin University, Changchun 130012, China*

[3]*Changchun Institute of Optics, Fine Mechanics and Physics, Chinese Academy of Sciences, Changchun 130025, China*

[4]*Department of Chemistry and Physics, Louisiana State University, Shreveport, LA 71115, USA*

[5]*wyu6000@gmail.com*

**yuzhang@jlu.edu.cn*

Abstract: The optical property variation induced by temperature change for PbSe quantum dot (QD)-filled hollow core fiber was investigated as a function of particle size, waveguide length, and doping concentration. The temperature coefficients of emission peak and intensity in QD-filled fiber were obviously size-dependent. The fiber filled with 4.5 nm PbSe QDs had better temperature stability in emission wavelength. The mechanism of the output loss in fiber was established, based on the thermal quenching of QD luminescence and the guided mode leakage arising from the temperature dependent refractive indexes of the fiber core and the cladding.

OCIS codes: (060.2290) Fiber materials; (160.4236) Nanomaterials; (060.2310) Fiber optics.

References and links

1. A. P. Alivisatos, "Perspectives on the physical chemistry of semiconductor nanocrystals," J. Phys. Chem. B **100**(31), 13226–13239 (1996).
2. A. P. Alivisatos, "Semiconductor clusters, nanocrystals, and quantum dots," Science **271**(5251), 933–937 (1996).
3. W. W. Yu, Y. A. Wang, and X. Peng, "Formation and stability of size-, shape-, and structure-controlled CdTe nanocrystals: ligand effects on monomers and nanocrystals," Chem. Mater. **15**(22), 4300–4308 (2003).
4. K. R. Choudhury, Y. Sahoo, T. Y. Ohulchanskyy, and P. N. Prasad, "Efficient photoconductive devices at infrared wavelengths using quantum dot-polymer nanocomposites," Appl. Phys. Lett. **87**(7), 073110 (2005).
5. W. W. Yu, L. Qu, W. Guo, and X. Peng, "Experimental determination of the extinction coefficient of CdTe, CdSe, and CdS nanocrystals," Chem. Mater. **15**(14), 2854–2860 (2003).
6. W. W. Yu, L. Qu, W. Guo, and X. Peng, "Experimental determination of the extinction coefficient of CdTe, CdSe and CdS nanocrystals: correction," Chem. Mater. **16**(3), 560 (2004).
7. W. W. Yu and X. Peng, "Formation of high-quality CdS and other II-VI semiconductor nanocrystals in noncoordinating Solvents: Tunable reactivity of monomers," Angew. Chem. Int. Ed. Engl. **41**(13), 2368–2371 (2002).
8. C. Cheng, "A multiquantum-dot-doped fiber amplifier with characteristics of broadband, flat gain, and low noise," J. Lightwave Technol. **26**(11), 1404–1410 (2008).
9. A. R. Bahrampour, H. Rooholamini, L. Rahimi, and A. A. Askari, "An inhomogeneous theoretical model for analysis of PbSe quantum-dot-doped fiber amplifier," Opt. Commun. **282**(22), 4449–4454 (2009).
10. C. Cheng, H. Jiang, D. Ma, and X. Cheng, "An optical fiber glass containing PbSe quantum dots," Opt. Commun. **284**(19), 4491–4495 (2011).
11. G. Springholz, T. Schwarzl, W. Heiss, G. Bauer, M. Aigle, H. Pascher, and I. Vavra, "Midinfrared surface-emitting PbSe/PbEuTe quantum-dot lasers," Appl. Phys. Lett. **79**(9), 1225–1227 (2001).
12. D. L. Huffaker, G. Park, Z. Zou, O. B. Shchekin, and D. G. Deppe, "1.3 μm room-temperature GaAs-based quantum-dot laser," Appl. Phys. Lett. **73**(18), 2564–2566 (1998).
13. C. Meng, Y. Xiao, P. Wang, L. Zhang, Y. Liu, and L. Tong, "Quantum-dot-doped polymer nanofibers for optical sensing," Adv. Mater. **23**(33), 3770–3774 (2011).
14. P. Jorge, M. Martins, T. Trindade, J. Santos, and F. Farahi, "Optical fiber sensing using quantum dots," Sensors (Basel Switzerland) **7**(12), 3489–3534 (2007).
15. K. Barnham, J. L. Marques, J. Hassard, and P. O'Brien, "Quantum-dot concentrator and thermodynamic model for the global redshift," Appl. Phys. Lett. **76**(9), 1197–1199 (2000).

#216853 - $15.00 USD Received 14 Jul 2014; revised 2 Aug 2014; accepted 2 Aug 2014; published 13 Aug 2014

16. S. M. Reda, "Synthesis and optical properties of CdS quantum dots embedded in silica matrix thin films and their applications as luminescent solar concentrators," Acta Mater. **56**(2), 259–264 (2008).
17. Q. Dai, Y. Wang, X. Li, Y. Zhang, D. J. Pellegrino, M. Zhao, B. Zou, J. Seo, Y. Wang, and W. W. Yu, "Size-dependent composition and molar extinction coefficient of PbSe semiconductor nanocrystals," ACS Nano **3**(6), 1518–1524 (2009).
18. F. W. Wise, "Lead salt quantum dots: the limit of strong quantum confinement," Acc. Chem. Res. **33**(11), 773–780 (2000).
19. H. Du, C. Chen, R. Krishnan, T. D. Krauss, J. M. Harbold, F. W. Wise, M. G. Thomas, and J. Silcox, "Optical properties of colloidal PbSe nanocrystals," Nano Lett. **2**(11), 1321–1324 (2002).
20. V. I. Klimov, A. A. Mikhailovsky, S. Xu, A. Malko, J. A. Hollingsworth, C. A. Leatherdale, H.-J. Eisler, and M. G. Bawendi, "Optical gain and stimulated emission in nanocrystal quantum dots," Science **290**(5490), 314–317 (2000).
21. J. S. Steckel, S. Coe-Sullivan, V. Bulović, and M. G. Bawendi, "1.3 μm to 1.55 μm tunable electroluminescence from PbSe quantum dots embedded within an organic device," Adv. Mater. **15**(21), 1862–1866 (2003).
22. A. Hreibi, F. Gérôme, J.-L. Auguste, Y. Zhang, W. W. Yu, and J.-M. Blondy, "Semiconductor-doped liquid-core optical fiber," Opt. Lett. **36**(9), 1695–1697 (2011).
23. L. Zhang, Y. Zhang, H. Wu, T. Zhang, P. Gu, H. Chu, T. Cui, Y. Wang, H. Zhang, J. Zhao, and W. W. Yu, "Multiparameter-dependent spontaneous emission in PbSe quantum dot-doped liquid-core multi-mode fiber," J. Nanopart. Res. **15**(10), 1–10 (2013).
24. A. Hartog, "A distributed temperature sensor based on liquid-core optical fibers," J. Lightwave Technol. **1**(3), 498–509 (1983).
25. G. B. Hocker, "Fiber-optic sensing of pressure and temperature," Appl. Opt. **18**(9), 1445–1448 (1979).
26. P. Gu, Y. Zhang, Y. Feng, T. Zhang, H. Chu, T. Cui, Y. Wang, J. Zhao, and W. W. Yu, "Real-time and on-chip surface temperature sensing of GaN LED chips using PbSe quantum dots," Nanoscale **5**(21), 10481–10486 (2013).
27. W. Liu, Y. Zhang, W. Zhai, Y. Wang, T. Zhang, P. Gu, H. Chu, H. Zhang, T. Cui, Y. Wang, J. Zhao, and W. W. Yu, "Temperature-dependent photoluminescence of ZnCuInS/ZnSe/ZnS quantum dots," J. Phys. Chem. C **117**(38), 19288–19294 (2013).
28. S. Li, K. Zhang, J.-M. Yang, L. Lin, and H. Yang, "Single quantum dots as local temperature markers," Nano Lett. **7**(10), 3102–3105 (2007).
29. Q. Dai, Y. Zhang, Y. Wang, M. Z. Hu, B. Zou, Y. Wang, and W. W. Yu, "Size-dependent temperature effects on PbSe nanocrystals," Langmuir **26**(13), 11435–11440 (2010).
30. A. Narayanaswamy, L. F. Feiner, and P. J. van der Zaag, "Temperature dependence of the photoluminescence of InP/ZnS quantum dots," J. Phys. Chem. C **112**(17), 6775–6780 (2008).
31. W. W. Yu, J. C. Falkner, B. S. Shih, and V. L. Colvin, "Preparation and characterization of monodisperse PbSe semiconductor nanocrystals in a noncoordinating solvent," Chem. Mater. **16**(17), 3318–3322 (2004).
32. Y. Zhang, Q. Dai, X. Li, Q. Cui, Z. Gu, B. Zou, Y. Wang, and W. W. Yu, "Formation of PbSe/CdSe core/shell nanocrystals for stable near-infrared high photoluminescence emission," Nanoscale Res. Lett. **5**(8), 1279–1283 (2010).
33. Y. Zhang, Q. Dai, X. Li, B. Zou, Y. Wang, and W. Yu, "Beneficial effect of tributylphosphine to the photoluminescence of PbSe and PbSe/CdSe nanocrystals," J. Nanopart. Res. **13**(9), 3721–3729 (2011).
34. Y. Zhang, Q. Dai, X. Li, J. Liang, V. L. Colvin, Y. Wang, and W. W. Yu, "PbSe/CdSe and PbSe/CdSe/ZnSe hierarchical nanocrystals and their photoluminescence," Langmuir **27**(15), 9583–9587 (2011).
35. O. E. Semonin, J. C. Johnson, J. M. Luther, A. G. Midgett, A. J. Nozik, and M. C. Beard, "Absolute photoluminescence quantum yields of IR-26 Dye, PbS, and PbSe quantum dots," J. Phys. Chem. Lett. **1**(16), 2445–2450 (2010).
36. G. Morello, M. De Giorgi, S. Kudera, L. Manna, R. Cingolani, and M. Anni, "Temperature and size dependence of nonradiative relaxation and exciton–phonon coupling in colloidal CdTe quantum dots," J. Phys. Chem. C **111**(16), 5846–5849 (2007).
37. K. A. Abel, H. Qiao, J. F. Young, and F. C. J. M. van Veggel, "Four-fold enhancement of the activation energy for nonradiative decay of excitons in PbSe/CdSe core/shell versus PbSe colloidal quantum dots," J. Phys. Chem. Lett. **1**(15), 2334–2338 (2010).
38. L. Zhang, Y. Zhang, S. V. Kershaw, Y. Zhao, Y. Wang, Y. Jiang, T. Zhang, W. W. Yu, P. Gu, Y. Wang, H. Zhang, and A. L. Rogach, "Colloidal PbSe quantum dot-solution-filled liquid-core optical fiber for 1.55 μm telecommunication wavelengths," Nanotechnology **25**(10), 105704 (2014).
39. S. Rieger, T. Hellwig, T. Walbaum, and C. Fallnich, "Optical repetition rate stabilization of a mode-locked all-fiber laser," Opt. Express **21**(4), 4889–4895 (2013).
40. H. L. Leertouwer, B. D. Wilts, and D. G. Stavenga, "Refractive index and dispersion of butterfly chitin and bird keratin measured by polarizing interference microscopy," Opt. Express **19**(24), 24061–24066 (2011).

1. Introduction

Semiconductor quantum dots (QDs) have attracted great attention for their unique electrical and optical properties determined by the evident quantum confinement effect [1–4]. Their band gaps can be accurately tuned over a wide energy range by changing their composition and particle size [5–7]. With these unique properties, QDs with high quantum yield show

#216853 - $15.00 USD Received 14 Jul 2014; revised 2 Aug 2014; accepted 2 Aug 2014; published 13 Aug 2014

great potentials on optical waveguide structures, such as amplifiers [8–10], lasers [11,12], sensors [13,14], and solar concentrators [15,16].

Among many types of QDs, PbSe QDs have become one of the most promising materials, whose exciton Bohr radius (46 nm) is much larger than that of cadmium systems (4-10 nm), providing strongly size-dependent property [17,18]. Its tunable band gap can cover the whole telecommunication waveband [18,19], which is a good material for optical fiber telecommunication. Owing to these unique properties, PbSe QD-doped optical waveguide structure has special potentials [20,21]. Hreibi *et al.* obtained emissions at 1220 nm with a 532 nm pump source coupling into a PbSe QD-doped liquid-core optical fiber [22]. Cheng *et al.* has proposed a PbSe QD-doped fiber amplifier with different particle sizes, which shows the characteristics of broader band, flatter gain, and lower noise [8]. Zhang *et al.* have established a theoretical model based on a three-level system model by combining the light propagation equations and the rate equations in order to calculate the guided spontaneous emission spectra of PbSe QD-filled fiber, which can be applied to both single- and multi-mode fibers [23]. However, the practical applications of QD-doped optical waveguide structure will be influenced by the surrounding environment [24,25], especially the environmental temperature. In addition, QDs have temperature-dependent optical properties [26–30], which make the study of the temperature effect on QD-doped optical waveguide structures necessary.

In this work, liquid-core fibers with an 18 cm-length heating area were fabricated by filling PbSe QDs with a series of particle sizes to investigate the temperature effect on the emission of QD-filled fiber. The output spectra at different temperatures were recorded to analyze the temperature effect for different QD particle sizes, fiber lengths, and doping concentrations, while the mechanisms of peak shift and intensity loss were confirmed.

2. Experiment

2.1 Synthesis of PbSe QDs

PbSe QDs were prepared based on the method reported by Yu *et al* [31,32]. In a typical synthesis, lead oxide (PbO, 0.892 g, 4.0 mmol), oleic acid (2.600 g, 8.0 mmol) and octadecene (ODE, 12.848 g) were mixed in a three necked flask and heated to 170 °C under N_2 until a clear solution was obtained. Then 6.9 mL selenium-trioctylphosphine solution (wt. 10% Se-TOP) was quickly injected into the flask and the mixture was cooled to 140 °C for QD growth. The reaction was stopped by injecting room-temperature toluene when the desired particle size was reached. The mixture was purified to remove excessive reaction precursors and solvents before the measurement, referring to the purification approach that has been well-established [27,33,34]. Methanol with an equal volume to the mixture was added to the sample solution in order to extract. The precipitated PbSe QDs were dissolved in hexane. Then excess acetone was added to the mixture to precipitate the QDs. After purification, the purified PbSe QDs were finally dispersed in tetrachloroethylene (TCE) for absorbance and other characterizations.

2.2 Material characterizations

A Perkin-Elmer Lambda 950 UV-Vis-NIR spectrometer and a Cary Eclipse spectrofluorimeter were respectively employed to record the absorption and photoluminescence (PL) spectra of PbSe QDs in TCE solvent. The QDs solution was sealed in nitrogen, and then heated to specific temperatures for 20 min to measure the corresponding optical spectra. Furthermore, the refractive indexes of PbSe QDs solution were obtained on a KRÜSS AR2008 Abbe refractometer.

2.3 Fabrication and measurement of the liquid-core fiber

The liquid-core optical fiber was fabricated by filling a hollow core fiber with PbSe QDs solution. The outer diameter and inner diameter of the hollow core fibers were 200 μm and 100 μm, respectively. First, a hollow core fiber with a required length was inserted into a

#216853 - $15.00 USD Received 14 Jul 2014; revised 2 Aug 2014; accepted 2 Aug 2014; published 13 Aug 2014

clean coupler. The QDs dissolved in TCE with known concentration were injected into the coupler using a syringe. The fiber was put under pressure until the QDs filled the whole fiber length to avoid production of air bubbles during the experiment. All the procedures and measurements were made under N_2 in a glove box. The fabricated fiber was heated to specific temperatures for the optical spectra measurement. We started such measurements at room temperature (23 °C) and then the temperature was set at 30, 40, 50, 60, 70, and 80 °C, respectively. When heated to a certain target temperature, the filled fiber was maintained for 10-20 min before measurements. A 532 nm continuous laser with a power of 200 mW was coupled into the liquid-core via a convex lens as shown in Fig. 1. The fiber output was characterized by an Omni-λ 3007 spectrometer.

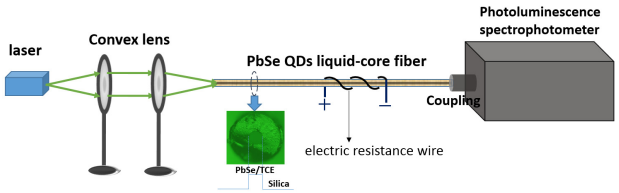

Fig. 1. A schematic diagram of PbSe QD-doped liquid-core fiber. Inset: optical image of a silica capillary filled with liquid nanoparticle solution (PbSe dissolved in tetrachloroethylene) and its equivalent step refractive index profile.

3. Results and discussion

Figure 2 shows the absorption and PL spectra of PbSe QDs with different particle sizes and the corresponding output spectra of liquid-core fiber; the length was 50 cm and the doping concentration was 7.2×10^{15} QD/cm^3 for all fibers. The emission peak has an obvious redshift after propagating through the 50 cm long fiber for all QDs sizes. This phenomenon is caused by the overlap between the absorption spectra and the emission band of the QDs (as seen in Figs. 2(a)-2(e)). During the guided emission propagation, some emitted photons at shorter wavelength from slightly smaller QDs due to the size distribution were reabsorbed by the slightly larger QDs and then new photons emitted at longer wavelength, resulting in a redshift of the emission peak [22]. As shown in Fig. 2(f), when temperature increased, the corresponding emission spectra of the fiber filling with 3.3 nm PbSe QD shifted to red, accompanied by a decrease of emission intensity. This temperature-induced redshift became less obvious as the particle size of PbSe QDs increased to 3.8 nm and 4.5 nm (Figs. 2(g) and 2(h)). When PbSe QDs became further larger (e.g., 4.9 nm in Fig. 2(i)), their emission spectra switched to blue shifts with the increase of temperature. These blue shifts became more apparent in Fig. 2(j), where the particle size was 5.8 nm.

As reported, there is a critical particle size of PbSe QDs whose spectra do not shift with the change of temperature; but when the size of PbSe QDs becomes relatively smaller or larger, spectra will shift to red or blue, respectively [29]. Therefore, this temperature-induced shift becomes less obvious as the size of PbSe QDs approaches to the critical particle size, which can also be seen in Fig. 3. Comparing to the temperature coefficient of PbSe QDs solution, there was a smaller temperature coefficient in the corresponding QD-filled liquid-core fiber (Fig. 3), which was mainly because the temperature-affected area was only part of the whole fiber. Therefore, there is less effect on emission wavelength. Even they do not have the same high quantum efficiency as the smaller size [35], 4.5 nm PbSe QDs with little temperature-dependence of emission peak are good candidate of waveguide medium, because they emit the photons of 1.55 μm telecommunication wavelength.

#216853 - $15.00 USD Received 14 Jul 2014; revised 2 Aug 2014; accepted 2 Aug 2014; published 13 Aug 2014

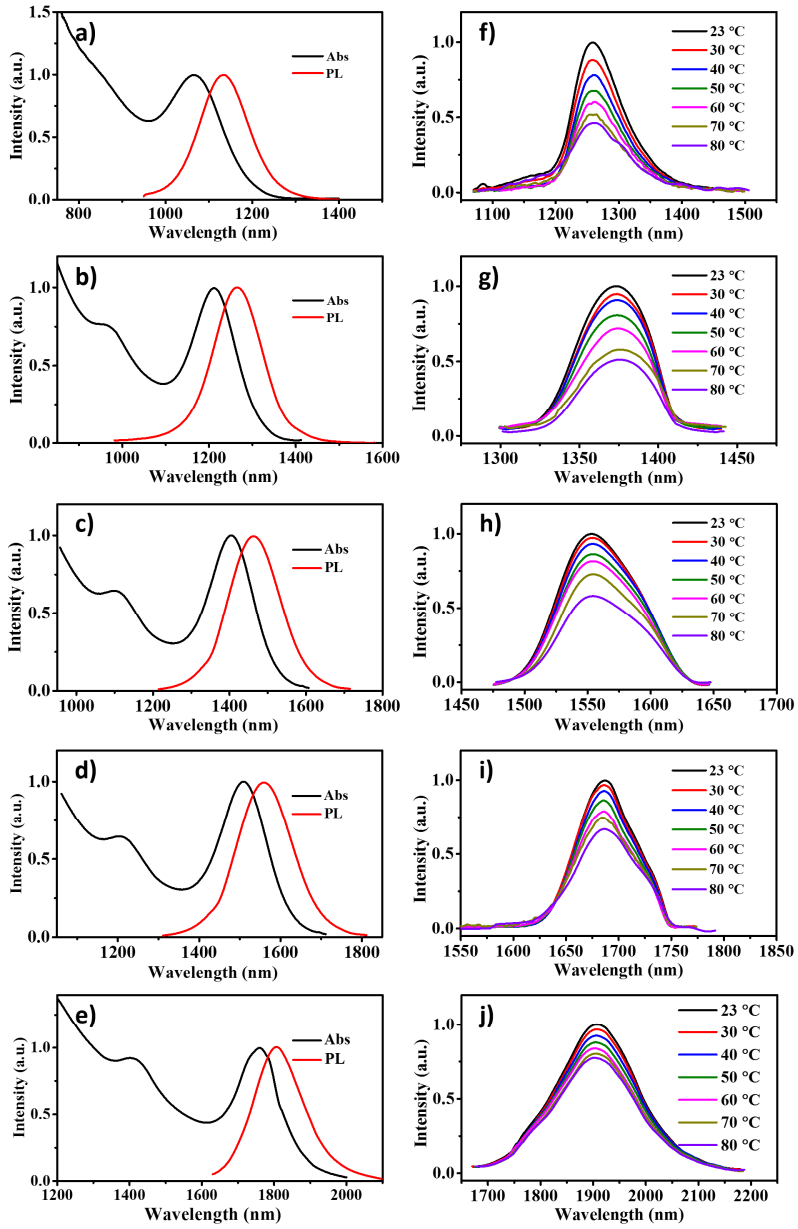

Fig. 2. Left panel: absorption and photoluminescence spectra recorded at room temperature for five different sizes PbSe QDs: (a) 3.3 nm; (b) 3.8 nm; (c) 4.5 nm; (d) 4.9 nm; (e) 5.8 nm. Right panel: the variations of filled fiber output spectra of different sizes at different temperatures: (f) 3.3 nm; (g) 3.8 nm; (h) 4.5 nm; (i) 4.9 nm; (j) 5.8 nm.

#216853 - $15.00 USD Received 14 Jul 2014; revised 2 Aug 2014; accepted 2 Aug 2014; published 13 Aug 2014

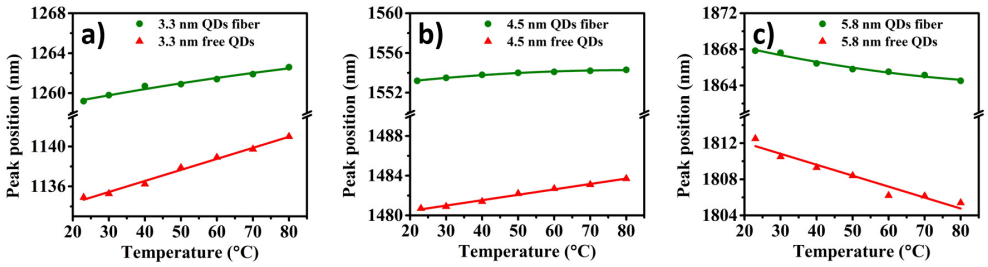

Fig. 3. The temperature-dependent emission peak position for different sizes of PbSe QDs solution and the PbSe QDs-filled liquid-core fibers: (a) 3.3 nm; (b) 4.5 nm; (c) 5.8 nm.

The emission intensity of PbSe QD-filled optical fiber decreases with the increasing temperature (Figs. 2(f)-2(j) and Figs. 4(a)-4(c)), which may be caused by thermal quenching of PbSe QDs according to the following equation [36]

$$I_{PL}(T) = \frac{I_0}{1 + A\exp(-\frac{E_a}{K_B T}) + B\left[\exp(\frac{E_{LO}}{K_B T}) - 1\right]^{-m}}, \quad (1)$$

where $I_{PL}(T)$ is the integrated PL intensity at temperature T; I_0 is the 0 K integrated PL intensity; E_a is the activation energy; and m is the number of exciton-longitudinal-optical (LO)-phonons involved in thermal escape of carriers and E_{LO} is their energy; A and B represent the probability ratios of the thermal activation and thermal escape to the radiative transition. The PL intensities of PbSe QDs with different sizes as a function of inverse k_BT are shown in Fig. 4(d). The fitting parameters listed in Table 1 are in good agreement with the previous work [37]. In our excitation regime (a few W/cm^2), the main recombination process in QDs include radiative recombination, thermal escape from the dot, and carriers localization at surface states [36]. Due to the enhancement of the exciton-phonon coupling with increased temperature, the non-radiative recombination will increase, causing the decrease of the emission intensity of PbSe QD-filled fiber.

Table 1. Fitting parameters based on Eq. (1)

PbSe sample	E_a (meV)	E_{LO} (meV)	m	A	B
3.3 nm	20.35	17.03	3.193	25.695	40.613
4.5 nm	18.32	17.01	3.153	15.695	40.613
5.8 nm	18.78	16.95	3.069	17.165	40.744

However, comparing to the temperature-dependent PL intensity of PbSe QDs in solution, the intensity attenuation ratio of fiber output is higher as shown in Figs. 4(a)-4(c), which indicates there must be temperature-induced loss mechanisms of the output intensity other than thermal quenching of QDs. According to the previous theoretical model, the distribution of the emission power along the radial direction satisfies the zero-order Bessel function and can be expressed as [23,38]

$$P_s(r_j, \lambda) = \left[\frac{J_0(V_j)}{J_0(V_1)}\right]^2 P_s(r_1), \quad (2)$$

where $P_s(r_1)$ is the emission power of the fundamental mode; V_j is the normalized frequency and is represented as

#216853 - $15.00 USD Received 14 Jul 2014; revised 2 Aug 2014; accepted 2 Aug 2014; published 13 Aug 2014

$$V_j = \frac{2\pi}{\lambda}\sqrt{n_{core}^2 - n_{clad}^2}\, r_j, \tag{3}$$

where n_{core} and n_{clad} are the refractive indexes of the core and the cladding of fiber, respectively. The total emission power of fiber cross section can be expressed as

$$P_s(\lambda) = \sum_{j=1}^{M} P_s(r_j, \lambda) = \frac{P_s(r_1)}{\left[J_0(V_1)\right]^2} \sum_{j=1}^{M} \left[J_0(V_j)\right]^2, \tag{4}$$

where M is the number of guided modes in fiber core and is expressed as

$$M(T) = \frac{4a^2}{\lambda^2}(n_{core}^2(T) - n_{clad}^2(T)), \tag{5}$$

where a is the core radius of the optical fiber; λ is the propagating light wavelength. Therefore, the emission intensity is proportional to the guided modes propagating in fiber, which are determined by the refractive indexes of both fiber core and cladding.

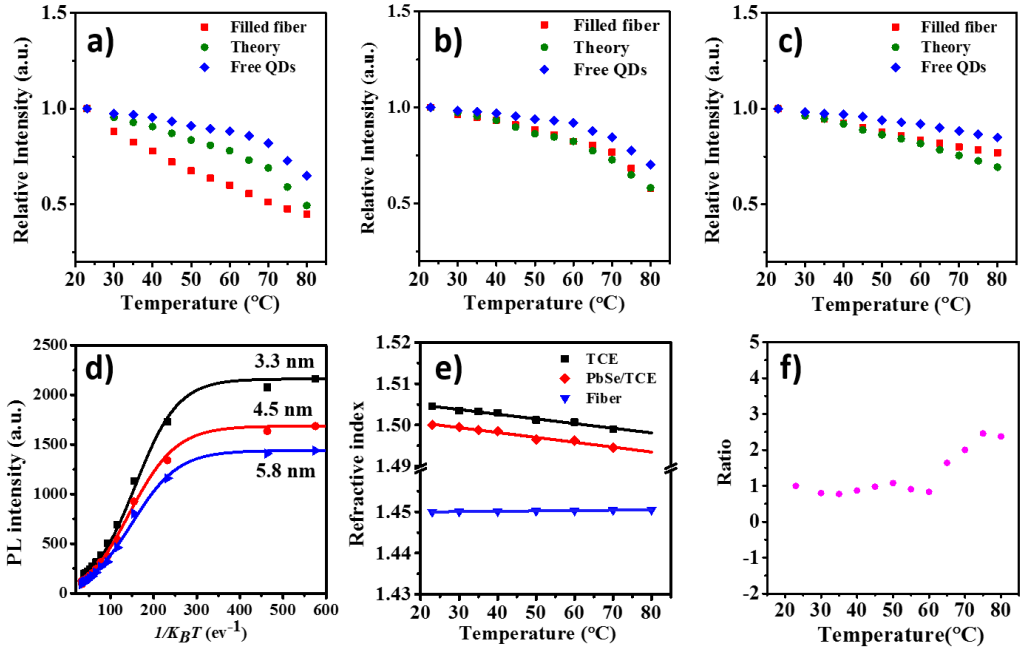

Fig. 4. Comparison between theoretical modeling and experimental results related to the output intensity of PbSe QD-filled liquid-core fibers and free QDs solution: (a) 3.3 nm, (b) 4.5 nm, (c) 5.8 nm; the integrated PL intensities of PbSe QDs with different particle sizes as a function of $1/k_BT$ (d); the refractive indexes of solvent TCE, PbSe QDs dissolved in TCE solvent and silica fiber at different temperatures (e); the ratio of the contribution to the decrease of emission intensity from thermal quenching to modes leakage for 4.5 nm QDs (f).

Figure 4(e) shows the measured refractive indexes of TCE and PbSe QDs solution at different temperatures, and the reported refractive indexes of silica fiber [39]. According to Eq. (5), the guided modes in fiber at different temperatures are calculated. The decrease of the refractive index of fiber core and increase of the refractive index of fiber cladding with the increasing temperature result in the weakening of guide confinement and leakage of guided modes. Therefore, considering the leakage of modes in fiber and thermal quenching of QDs with the increasing temperature, the decrease trend of the calculated relative intensity in fiber at different temperatures is in accordance with the measured one (Figs. 4(a)-4(c)). Based on

#216853 - $15.00 USD Received 14 Jul 2014; revised 2 Aug 2014; accepted 2 Aug 2014; published 13 Aug 2014

the above analysis, it can be concluded that there are two main factors resulting in the temperature-induced change of output intensity of PbSe QD-filled fiber, the thermal quenching effect of QDs and guided modes leakage in fiber. By calculating the ratio of the contribution to the decrease of emission intensity from thermal quenching to modes leakage (Fig. 4(f)), it can be concluded that the contributions from the two effects were almost equal at the temperature from 20 to 60 °C, while the effect of mode leakage is less dominant for high temperature because the temperature coefficient of the number of guided mode decreases with the increased temperature according to Eq. (5). In addition, the intensity attenuation ratio of the output of PbSe QD-filled fiber is also size-dependent, which become lower with the increase of particle size, as shown in Figs. 2(f)-2(j). The low-order modes would hardly be affected in fiber, while the high-order modes would be strongly affected. Photons with long wavelengths emitted by large size QDs have relative low refractive index [40]. Therefore, for large size QDs solution with low refractive index (Table 2), most of emitted power is confined in low-order modes in fiber, which induces a better stability of long distance propagating and leads to the weaker temperature effect and smaller attenuation ratio of the emission power for large size QD-filling fiber.

Table 2. Refractive index of PbSe/TCE solution with different particle sizes and the same concentration of 7.2×10^{15} QDs/cm^3 at room temperature

QD size (nm)	3.3	4.5	5.8
Refractive index	1.5035	1.5000	1.4975

The temperature effect of output spectra of 4.5 nm PbSe QD-filled fibers with different fiber lengths and QD doping concentrations are further investigated. Three fiber lengths (36, 50, and 80 cm) were chosen to analyze the length dependence of the temperature effect on the emission of liquid-core fiber, with the same doping concentration. Due to the guided spontaneous emission in the fiber and the reabsorption and emission effect, the emission peaks shift red with the increase of fiber length [22,38]. Figure 5(a) shows that the emission peaks of fibers with different lengths shifts to red in a similar trend with the increased temperature, which also further demonstrates the good temperature stability of emission wavelength for 4.5 nm QD-doped fiber. As shown in Fig. 5(b), the temperature coefficients of emission relative intensity become smaller with the fiber length increased from 36 to 80 cm. The fiber length-dependent temperature effect of emission intensity is mainly due to the fixed length of heating area. The guided modes outside the heating area of the fiber propagate at room temperature without extra leakage. Therefore, the temperature coefficients of emission relative intensity are proportional to the ratio of the fixed length of heating area to the whole fiber. This demonstrates that for a long QD-filled waveguide, the temperature-induced variation of output intensity is very weak with a fixed length of heating area.

#216853 - $15.00 USD Received 14 Jul 2014; revised 2 Aug 2014; accepted 2 Aug 2014; published 13 Aug 2014

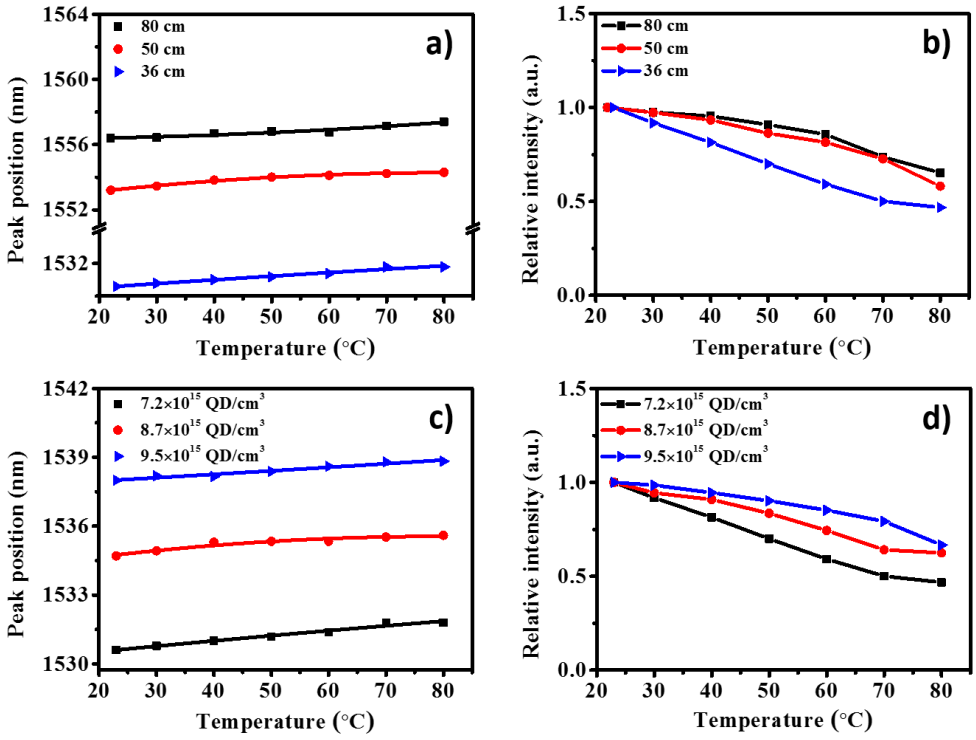

Fig. 5. The temperature-dependent emission peak positions (a) and intensity (b) of 4.5 nm PbSe QD-filled fibers with different fiber lengths; the temperature-dependent emission peak positions (c) and intensity (d) of 4.5 nm PbSe QD-filled fibers with different doping concentration.

Moreover, the temperature-dependent output spectra of fibers were recorded with different PbSe QDs doping concentrations of 7.2×10^{15}, 8.7×10^{15}, and 9.5×10^{15} QD/cm^3, with the same fiber length of 36 cm. The emission peak shifted to red at roughly the same rate of about 0.021 nm/°C when temperature increased for different doping concentrations, as shown in Fig. 5(c). Figure 5(d) shows that the attenuation ratio of fiber output emission intensity decreases with the increase of QD doping concentration. The refractive indexes of PbSe QDs solutions with different doping concentrations of 7.2×10^{15}, 8.7×10^{15}, and 9.5×10^{15} QD/cm^3 were measured to be 1.5000, 1.4995 and 1.4990, respectively, at room temperature (Table 3). The low-order mode would hardly be affected, while the high-order modes would be strongly affected. For the optical waveguide structure with small difference of relative refractive indexes, most emitted power is confined in low-order modes, which have better stability of long distance propagating, leading to the weak temperature effect and small attenuation ratio of the emission power at high doping concentration.

Table 3. Refractive index of PbSe/TCE solution with the different concentrations and the same particle size of 4.5 nm at room temperature

Concentration (× 10^{15} QD/cm^3)	7.2	8.7	9.5
Refractive index	1.5000	1.4995	1.4990

4. Conclusions

In summary, we have characterized the temperature effect of PbSe QD solution-filled liquid-core fibers with different particle sizes. The QD size dependence of temperature effect of

#216853 - $15.00 USD Received 14 Jul 2014; revised 2 Aug 2014; accepted 2 Aug 2014; published 13 Aug 2014

output spectra in liquid-core fiber was observed, which demonstrated that 4.5 nm PbSe QDs were better waveguide medium due to the good stability of output peak wavelength. Additionally, by analyzing the light propagation equations and rate equations, the loss mechanisms of fiber output intensity were concluded, including the thermal quenching of PbSe QDs solution and the guided modes leakage in fiber. Finally, the temperature effect of PbSe QD-doped fiber with different fiber lengths, QD doping concentrations were also investigated, which confirmed that PbSe QD-filled optical fibers with long fiber length and high doping concentration have better stability of output intensity with the change of temperature. This study can lay a foundation for the future application of the QD-filled optical waveguide structure, such as amplifiers, lasers, and telecommunication.

Acknowledgments

This work was financially supported by the National 863 Program (2011AA050509), the National Natural Science Foundation of China (61106039, 51272084, 61306078, and 61225018), the National Postdoctoral Foundation (2011049015), the Jilin Province Key Fund (20140204079GX), the Hong Kong Scholar Program (XJ2012022), the State Key Laboratory on Integrated Optoelectronics (IOSKL2012ZZ12), NSF (CHE-1338346), and 3M Faculty Award.

#216853 - $15.00 USD Received 14 Jul 2014; revised 2 Aug 2014; accepted 2 Aug 2014; published 13 Aug 2014